THE ASTROPHYSICAL JOURNAL LETTERS, IN PRESS
Preprint typeset using LaTeX style emulateapj v. 7/8/03

arXiv:astro-ph/0310039v1 1 Oct 2003

CHANDRA AND HST CONFIRMATION OF THE LUMINOUS AND VARIABLE X-RAY SOURCE IC 10 X-1 AS A POSSIBLE WOLF-RAYET, BLACK-HOLE BINARY

FRANZ E. BAUER[1] AND W. N. BRANDT[1]

(Received 2003 July 20; Accepted 2003 September 26)
The Astrophysical Journal Letters, in press

ABSTRACT

We present a *Chandra* and *HST* study of IC 10 X-1, the most luminous X-ray binary in the closest starburst galaxy to the Milky Way. Our new hard X-ray observation of X-1 confirms that it has an average 0.5–10 keV luminosity of 1.5×10^{38} erg s^{-1}, is strongly variable (a factor of $\approx$2 in $\lesssim$3 ks), and is spatially coincident (within $0\farcs23\pm0\farcs30$) with the Wolf-Rayet (WR) star [MAC92] 17A in IC 10. The spectrum of X-1 is best fit by a power law with $\Gamma\approx1.8$ and a thermal plasma with $kT\approx1.5$ keV, although systematic residuals hint at further complexity. Taken together, these facts suggest that X-1 may be a black hole belonging to the rare class of WR binaries; it is comparable in many ways to Cyg X-3. The *Chandra* observation also finds evidence for extended X-ray emission co-spatial with the large non-thermal radio superbubble surrounding X-1.

Subject headings: galaxies: individual: IC 10 — X-rays: binaries — stars: Wolf-Rayet — X-rays: ISM

1. INTRODUCTION

IC 10 is a metal-poor ($Z\approx0.15Z_\odot$; Lequeux et al. 1979), barred dwarf irregular in the Local Group. Although hampered by uncertain reddening corrections, reliable optical and infrared distance estimates place IC 10 at 0.6–0.8 Mpc (e.g., Saha et al. 1996; Sakai et al. 1999; Borissova et al. 2000; we adopt 0.7 Mpc), indicating that it is the nearest starburst galaxy to the Milky Way. IC 10 is notable for its vigorous star formation ($\approx$0.03 $M_\odot$ yr^{-1} kpc^{-2}; e.g., Hunter & Gallagher 1986; Thronson et al. 1990; Hunter et al. 1993) and unusually large massive (OB) star population, including a *galaxy-wide* surface density of Wolf-Rayet (WR) stars $\gtrsim$4 times that observed in the most active regions of star formation in *any* other Local Group galaxy (Massey & Johnson 1998; Royer et al. 2001; Crowther et al. 2003). This ongoing star formation in IC 10 is expected to result in copious X-ray emission, both from compact high-mass X-ray sources and supernova-heated gas. The galaxy was observed twice using the *ROSAT* HRI in 1996 (70.3 ks combined exposure), although the X-ray flux in the HRI band is diminished by a factor of $\approx$5 due to the Galactic column of 4.8×10^{21} cm^{-2} (Stark et al. 1992) and the expected absorption internal to IC 10 of $\approx2\times10^{21}$ cm^{-2} (e.g., Yang & Skillman 1993). One highly significant source was previously detected (hereafter X-1) within the optical extent of IC 10 (Brandt et al. 1997). This source was found to vary by a factor of $\approx$3 on $\sim$1 day timescales, with an average absorbed HRI flux of 4×10^{-13} erg cm^{-2} s^{-1} (or an unabsorbed $L_{0.1\text{–}2.5\ \mathrm{keV}}\approx7\times10^{37}$ erg s^{-1}). The HRI-derived position (5″ rms) placed X-1 in a region with intense star formation as well as the most massive H I cloud in IC 10. Notably, X-1 was found to lie $\approx2''$ from [MAC92] 17 ($V=21.76$), an emission-line source identified as a WR star by Massey et al. (1992) and Crowther et al. (2003), and within $\approx8''$ of the centroid of a non-thermal radio superbubble ($\approx45''$/150 pc diameter; Yang & Skillman 1993). The combination of the high X-ray luminosity and strong variability argued that X-1 is a powerful X-ray binary (containing a neutron star or black hole).

In this Letter we report on *Chandra* and *HST* follow-up observations of IC 10 that further characterize the nature of X-1. In particular, these observations more accurately determine the X-ray luminosity and spectrum of X-1 (both of which were uncertain since the *ROSAT* HRI had essentially no spectral capability and was affected by the large absorption) and confirm the likely association of X-1 and the WR star [MAC92] 17 (there are several potential optical counterparts to X-1 within the 5″ radius HRI error circle). In §2 we outline the relevant X-ray and optical observations and analyses, while in §3 we summarize our findings and discuss X-1 in the broader context of black-hole binaries (BHBs).

2. OBSERVATIONS AND ANALYSIS

2.1. *Chandra Observations*

IC 10 was observed on 2003 March 12 with ACIS-S (the spectroscopic array of the Advanced CCD Imaging Spectrometer; Garmire et al. 2003). To limit telemetry saturation in the case of high background, only chips S2 and S3 in the ACIS-S array were operated, while a 500-pixel subarray was used to lower the frame time to 1.7 s and thus limit potential pileup of X-1. Events were telemetered in Very Faint (VF) mode, and the CCD temperature was −120° C. The optical extent of IC 10 ($\approx6\farcm3\times5\farcm1$) is only marginally cropped by the 2-chip, 500-pixel subarray configuration ($16\farcm8\times4\farcm1$).

Analysis was performed using the CIAO software (v2.3) provided by the *Chandra* X-ray Center (CXC), but also with FTOOLS (v5.2) and custom IDL software. The data were corrected for the radiation damage sustained by the CCDs during the first few months of *Chandra* operations using the Charge Transfer Inefficiency (CTI) correction procedure of Townsley et al. (2002).[2] Following CTI-correction, the data were reprocessed with the CIAO tool ACIS_PROCESS_EVENTS to remove the standard $0\farcs5$ pixel randomization and to flag potential ACIS background events using VF mode screening. We performed standard *ASCA* grade selection in the 0.3–8.0 keV band, excluding all bad columns, bad pixels, VF-mode background events, and cosmic-ray afterglows. We used only data taken during times within the CXC-generated good-time intervals. The background varied by $<$30% during the observation, with the average background rate being 2.2×10^{-7} counts s^{-1} pixel^{-1} and

[1] Department of Astronomy & Astrophysics, 525 Davey Lab, The Pennsylvania State University, University Park, PA 16802.

[2] For details see http://www.astro.psu.edu/users/townsley/cti/.

7.0×10^{-7} counts s^{-1} $pixel^{-1}$ on chips S2 and S3, respectively (in agreement with ACIS quiescent-background calibration measurements).[3] The total net exposure time is 29,191 s.

X-ray sources were identified using the CIAO wavelet algorithm WAVDETECT (Freeman et al. 2002) on the 0.3–8.0 keV (full), 0.3–2.0 keV (soft), and 2.0–8.0 keV (hard) images with a probability threshold of 10^{-6}. In total, 43 sources were detected. The positions, counts, and spectra for these sources were derived using ACIS_EXTRACT (AE; Broos et al. 2002) with 95% encircled-energy radii [based on point spread functions (PSFs) from MKPSF and the PSF library]; the adopted X-ray source positions were found using the matched-filter method within AE.

2.2. *HST Observations*

To compare the X-ray and optical emission, we observed IC 10 with the *HST* Advanced Camera for Surveys (ACS; Ford et al. 1998) on 2002 October 12. IC 10 was imaged along its major axis ($\approx 50°$) using two ACS pointings separated by 130″. Each pointing consisted of ≈ 0.5-orbit exposures in the *BVI* bands (F435W, F555W, F814W). The standard pipeline data products were used, although we mosaiced the two pointings ourselves due to a problem with the pipeline MULTIDRIZZLE procedure. Optical source positions and magnitudes were measured using SEXTRACTOR (v2.2.1; Bertin & Arnouts 1996).

2.3. *Astrometry of Optical and X-ray Images*

Due to the small number of X-ray sources that overlap the ACS field of view, we aligned both datasets to the set of high-quality ground-based images available from the NOAO archive for IC 10 (PI: Massey). Briefly, the NOAO images were matched to 55 GSC2.2 sources within 10′ of IC 10 ($\Delta\alpha = 0\farcs20$, $\Delta\delta = -0\farcs26$), giving an rms scatter of 0.″19; this alignment was confirmed using 11 Tycho 2 stars (0.″26 rms). Given the optical source density in the IC 10 region and apparent small, systematic field distortions in the NOAO images, we only matched 332 *HST* sources brighter than $B = 23$ within a 1.′5 region of X-1 ($\Delta\alpha = 5\farcs32$, $\Delta\delta = 0\farcs27$). This gives an astrometric accuracy of 0.″10 rms for the *HST* positions within the vicinity of X-1. Finally, 14 of the 43 significant X-ray sources (including X-1) have plausible optical counterparts, whereas only two false matches are expected. Aligning the X-ray and optical images ($\Delta\alpha = -0\farcs44$, $\Delta\delta = 0\farcs53$) yields an astrometric accuracy of 0.″28 rms for the X-ray positions.

2.4. *X-ray Analysis*

IC 10 X-1 has 4403 counts in the full band and, based on our astrometric solutions, it has a J2000 position of $\alpha = 00^{h}20^{m}29\fs09$, $\delta = +59°16'51\farcs95$. X-ray contours of X-1 are shown in Fig. 1 overlaid on the *HST* ACS F814W image. The Fig. 1 inset indicates the *Chandra* positional uncertainty of X-1, which is an order of magnitude smaller than found previously with the *ROSAT* HRI. X-1 lies 0.″23 from J002029.1+591652.1 (an $I_{AB} = 21.8$ WR star identified as [MAC92] 17 by Massey et al. 1992 and [MAC92] 17A by Crowther et al. 2003), 0.″33 from J002029.0+591651.6 ($I_{AB} = 24.4$), 0.″37 from J002029.1+591651.7 ($I_{AB} = 24.0$), and 0.″42 from J002029.0+591651.8 (an $I_{AB} = 21.8$ OB supergiant identified as [MAC92] 17B by Clark et al. 2003). Given the astrometric uncertainty in both the *HST* and *Chandra* coordinate frames (i.e., 0.″30, much larger than the individual centroiding errors), X-1 is most likely associated with [MAC92] 17A. Although we cannot exclude entirely an association with the latter sources (or fainter undetected sources) based on the astrometric errors, the probability of X-1 lying within 0.″23 of a WR star by chance is ≈0.05–0.2%.[4]

In addition to an X-ray point source in Fig. 1, we found faint extended X-ray emission roughly centered on X-1 and co-spatial with the Yang & Skillman (1993) non-thermal radio superbubble (see Fig. 1). This X-ray emission extends out to ∼20″ in the adaptively smoothed image. Given that the X-ray emission appears azimuthally symmetric to ∼15″, we extracted soft and hard-band counts around X-1 in 1-pixel an-

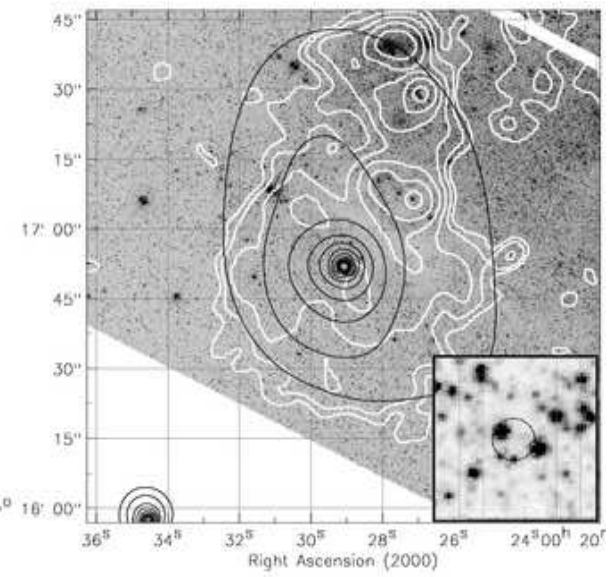

FIG. 1.— X-ray (dark) and radio (light) contours in the vicinity of X-1 overlaid on the *HST* ACS F814W image. The image shows X-1 in relation to the X-ray and radio emission from the surrounding superbubble. *Inset:* 50-pixel (≈2.″2) close-up of X-1 indicating the 0.″30 X-ray error circle (statistical+systematic) relative to the ACS F814W counterparts. X-1 lies 0.″23 from the confirmed WR star [MAC92] 17A (slightly above and to the left of the X-ray centroid; Crowther et al. 2003).

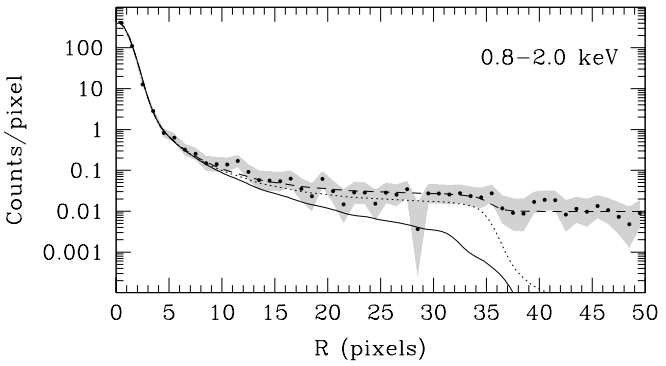

FIG. 2.— The 0.8–2.0 keV ACIS-S radial profile (small filled circles) of X-1, compared to our simple model with and without background (dashed and dotted curves, respectively) and the *Chandra* on-axis PSF (solid curve) calculated at 1.5 keV (i.e., closest to where the spectrum of X-1 peaks). The shaded region indicates the 1σ deviation of the measured profile. Deviations from the PSF can be seen out to radii of ≈35 pixels above 0.8–2.0 keV background of 0.010 counts $pixel^{-1}$. A pixel is equivalent to 0.″492.

[3] See http://cxc.harvard.edu/contrib/maxim/bg/index.html.

[4] Narrow-band photometric observations of IC 10 have identified ∼ 100 WR stars, of which 26 have been spectroscopically confirmed (Massey & Armandroff 1995; Royer et al. 2001; Crowther et al. 2003).

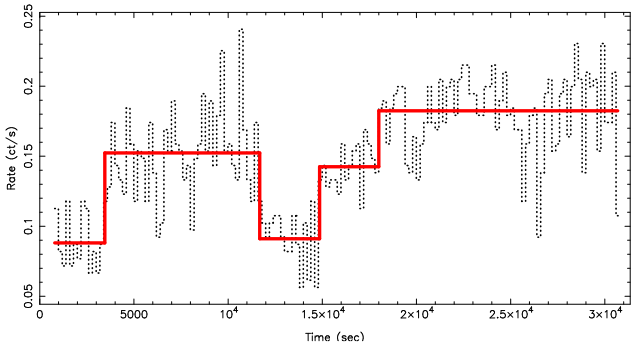

FIG. 3.— X-ray light curve of IC 10 X-1 (dotted) overlaid with the 99.9% confidence level Bayesian "blocks" of constant count rate (solid). The events are shown in 200 s bins.

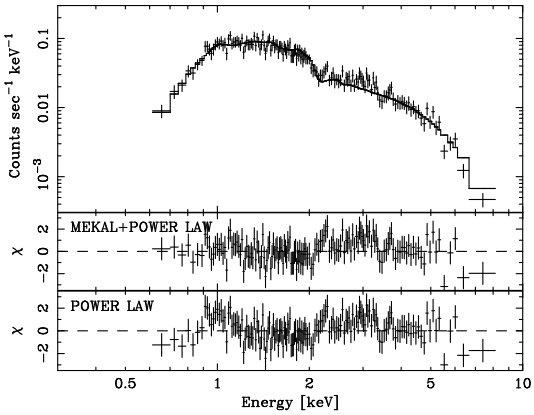

FIG. 4.— X-ray spectrum of the IC 10 X-1 point source, modeled with an absorbed power law and thermal plasma with Γ = 1.83, kT = 1.49 keV, and $N_{\rm H} = 6.0 \times 10^{21}$. Note the large residuals around 2.25 keV and 3.65 keV suggesting the presence of possible emission lines.

nular bins. Due to the large foreground absorption column of IC 10, we used the 0.8–2.0 keV band to reduce background where we detect no signal. For comparison, we generated the on-axis ACIS-S PSF using CHART,[5] extracting counts in an identical manner to the data. The radial surface-brightness distributions and 1σ errors for the data are shown in Fig. 2 and demonstrate that X-1 lies systematically above the background out to radii of $\sim$35 pixels ($\sim 17''$) and is clearly extended compared to the PSF model. The hard-band profile is consistent with a point source and background only.

We find 175 (129) counts in the full (soft) band between radii of 7–35 pixels (note that contamination from X-1 should be $< 1\%$ at such radii). The fact that the extended emission is present almost exclusively in the soft band further supports the reality of the extent. An emission model consisting of both a point source and a uniform disk with a $17''$ (60 pc) radius convolved with the PSF represents the 0.8–2.0 keV surface-brightness distribution well, although there is clearly still some residual scatter due to possible clumping. The flux ratio of the extended disk component to the point source is $\approx 2\%$. The relative softness of the extended emission is consistent with a physical origin as supernova-heated hot gas (see also the X-ray spectral analysis below).

Brandt et al. (1997) found that X-1 varied by a factor of $\approx$3 during their *ROSAT* HRI observation but did not have the statistics or the time sampling to constrain the variability further. With $\approx$4400 counts over a contiguous 29.2 ks, our light curve probes the short-term temporal properties better. A Kolmogorov-Smirnov test indicates that X-1 is variable at the $> 99.9\%$ confidence level. To derive the amplitude and characteristic timescale of variability, we used the Bayesian Block method provided in the contributed CIAO software package SITAR.[6] Fig. 3 shows a binned light curve of X-1, overplotted with a series of contiguous "blocks" within which the count rate is modeled as a constant at the 99.9% confidence level. X-1 has peak, trough, and average count rates of 0.182 ct s^{-1}, 0.088 ct s^{-1}, and 0.151 ct s^{-1}, respectively, and exhibits rapid variability by as much as a factor of $\approx$2 in $\lesssim$3000 s. The hardness ratio, however, shows no significant spectral variability. Since a significant fraction of X-ray binaries are X-ray pulsars with pulse periods ranging from 0.01–1,000 s (e.g., White et al. 1995), we generated power spectra to search for pulsations using the robust z_1^2 method (e.g., Buccheri et al. 1983). These power spectra also allowed us to search for other periodic phenomena (e.g., eclipses or regular X-ray bursts). No periodic behavior was found.

The X-ray spectra were analyzed using XSPEC (v11.2; Arnaud 1996). Unless stated otherwise, spectral parameter errors are for the 90% confidence level, assuming one parameter of interest. The X-ray fluxes and absorption-corrected luminosities for X-1 were calculated from the spectral fitting. For the detected X-1 count rates above, pile-up is estimated to be $\approx$15%. Thus, spectral analysis of this source must proceed with care. To model the spectrum in the presence of such pile-up, we used the forward-modeling tool LYNX developed at PSU (Chartas et al. 2000). The ACIS spectrum of X-1 was initially fit with an absorbed power-law model, giving best-fit values of $N_{\rm H} = (5.1 \pm 0.4) \times 10^{21}$ cm^{-2} and $\Gamma = 1.77 \pm 0.08$ (χ^2 = 97.6 for 82 degrees of freedom). The χ^2 value and apparent systematic residuals (bottom panel in Fig. 4) indicate the model provides a poor fit to the data. Given that we detect a low-level extended component around X-1, we added an absorbed thermal plasma component (*mekal*; e.g., Mewe et al. 1985) to our spectral model. The resulting best-fit values are $N_{\rm H} = (6.0^{+0.20}_{-0.08}) \times 10^{21}$ cm^{-2} (in agreement with the expected Galactic+intrinsic absorption), $\Gamma = 1.83^{+0.07}_{-0.11}$, and $kT = 1.49^{+0.15}_{-0.12}$ keV (χ^2 = 61.6 for 80 degrees of freedom). The abundances were not well constrained and were fixed at $Z = 0.15 Z_\odot$ (see §1). While this model provides a significant improvement to both the χ^2 value (>99.99% based on the F-test) and the apparent systematic residuals below $\sim$2 keV, there are still notable residuals around 2–4 keV (see middle panel in Fig. 4). These residuals, particularly around 2.25 keV and 3.65 keV, are perhaps due to marginally-resolved emission lines from an X-ray-photoionized wind (e.g., as seen in Cyg X-3; see §3). The 0.5–8.0 keV absorbed flux and unabsorbed luminosity of X-1, corrected for pileup, are 1.57×10^{-12} erg cm^{-2} s^{-1} and 1.50×10^{38} erg s^{-1}, respectively. The thermal component contributes $\approx$20% of the total absorbed flux and $\approx$27% of the total unabsorbed luminosity, which is substantially more than was estimated from fitting the radial profile. This suggests that either much of this component arises from X-1 itself or that the extended component is strongly centrally peaked rather than uniformly distributed. We also analyzed the spectrum of the extended X-ray component ($3\farcs5$–$17''$annulus around X-1). Given the small number of counts in this region, we modeled its spectrum using the Cash statistic (Cash 1979) instead of χ^2. An ab-

[5] See http://asc.harvard.edu/chart/.
[6] See http://space.mit.edu/CXC/analysis/SITAR/index.html

sorbed *mekal* model with fixed $N_{\rm H} = 5.9 \times 10^{21}$ cm^{-2} (as found for X-1) gives abest-fit temperature of $kT = 0.87^{+0.17}_{-0.21}$ keV. The 0.5–8.0 keV absorbed flux and unabsorbed luminosity of this extended component are 1.73×10^{-14} erg cm^{-2} s^{-1} and 3.24×10^{36} erg s^{-1}, respectively. This flux is consistent with our radial-profile fitting and supports an origin as hot gas associated with the radio superbubble.

3. DISCUSSION

This *Chandra* observation of IC 10 has resulted in improvements by factors of ≈15 in terms of spatial resolution and astrometric accuracy and ≈10 in terms of statistics for X-1, compared to previous *ROSAT* HRI exposures, allowing substantially better constraints to be placed on the nature of this object. The combination of the high luminosity and strong variability clearly demonstrates that X-1 is a powerful X-ray binary, containing a black hole or neutron star. Its likely physical association with [MAC92] 17A implies that the progenitor of X-1 must have evolved even more rapidly and been more massive than [MAC92] 17A (WNE stars typically have $M \approx 40$–$50 M_\odot$ and $t_{\rm life} \lesssim 5$ Myr; e.g., Maeder & Meynet 1994). Thus, we expect X-1 to be a BHB (although we note that there are clear counter examples; see, e.g., Kaper et al. 1995). Optical spectroscopic monitoring of X-1 to search for variability would be one of the best methods to prove the WR-BHB interpretation; Clark et al. (2003) find hints of variability in the λ4686 feature of [MAC92] 17A, but longer dedicated observations are needed to secure this finding.

The X-ray spectrum of X-1 is acceptably fit with a $\Gamma = 1.83$ power law and $kT = 1.49$ keV thermal plasma (potentially indicative a BHB in a hard state; e.g., McClintock & Remillard 2003). The residuals of X-1 in the 2–4 keV range hint at further spectral complexity, perhaps from emission lines or absorption features. Longer *Chandra* or *XMM-Newton* observations of X-1 would also be useful to quantify the origin of the spectral residuals, as well as to place additional constraints on the nature of the X-ray emission (e.g., to rule out further the presence of pulsations or bursts).

The properties of X-1 bear several similarities to the Galactic X-ray binary Cyg X-3 in terms X-ray luminosity, spectrum, and variability (e.g., Kitamoto et al. 1994; Liedahl & Paerels 1996; Predehl et al. 2000) as well as donor type (WNE vs. WN7; van Kerkwijk et al. 1996; Crowther et al. 2003). Moreover, Cyg X-3 has a complex X-ray spectrum including numerous emission lines and a 9 keV edge that are attributed to an X-ray-photoionized wind; the residuals seen from X-1 may have a similar origin. Thus IC 10 X-1 is the only other confirmed example of the short-lived WR X-ray binary.

The discovery of soft extended emission co-spatial with the large non-thermal radio superbubble surrounding X-1 is important for determining the nature of the bubble, although the poor statistics obtained here do not allow strong constraints. Obvious comparisons can be made with 30 Doradus (Dennerl et al. 2001), as well as with SS433/W50 (Safi-Harb & Oegelman 1997) and IC 342 X-1 (Roberts et al. 2003), all of which have similar physical extents and radio/X-ray luminosities as the bubble in IC 10. While the radio and X-ray emission from the IC 10 bubble is consistent with multiple supernovae, the superbubble does lie off the Σ–d relation (Yang & Skillman 1993), suggesting that something else (perhaps X-1) may be powering the expansion. For instance, in the case of W50, SS 433 is believed to contribute to the expansion. High-resolution radio imaging of IC 10 could be used to search for any jets associated with X-1 and explore whether X-1 has had any influence on the nonthermal superbubble.

We thank L. Townsley and M. van Kerkwijk for several helpful discussions, G. Chartas for help with the forward-modeling of the X-ray spectrum, M. Muno for help with variability constraints, S. Clark and P. Crowther both for interesting discussions regarding X-1 and communicating their results prior to publication. We gratefully acknowledge the financial support of CXC grant GO3-4112X (FEB, WNB), STScI grant HST-GO-09683.01A (FEB, WNB) and NASA LTSA grant NAG5-13035 (WNB).

REFERENCES

Arnaud, K. A. 1996, in ASP Conf. Ser. 101: Astronomical Data Analysis Software and Systems V, vol. 5, 17–20
Bertin, E. & Arnouts, S. 1996, A&AS, 117, 393
Borissova, J., et al. 2000, A&A, 363, 130
Brandt, W. N., Ward, M. J., Fabian, A. C., & Hodge, P. W. 1997, MNRAS, 291, 709
Broos, P., Townsley, L., Getman, K., & Bauer, F. 2002, ACIS Extract, An ACIS Point Source Extraction Package, Pennsylvania State University, http://www.astro.psu.edu/xray/docs/TARA/ae_users_guide.html
Buccheri, R., et al. 1983, A&A, 128, 245
Cash, W. 1979, ApJ, 228, 939
Chartas, G., et al. 2000, ApJ, 542, 655
Clark, J. S., Crowther, P. A., & Abbott, J. B. 2003, MNRAS, submitted
Crowther, P. A., et al. 2003, A&A, 404, 483
Dennerl, K., et al. 2001, A&A, 365, L202
Ford, H. C., et al. 1998, in Proc. SPIE Vol. 3356, p. 234-248, Space Telescopes and Instruments V, Pierre Y. Bely; James B. Breckinridge; Eds., 234–248
Freeman, P. E., Kashyap, V., Rosner, R., & Lamb, D. Q. 2002, ApJS, 138, 185
Garmire, G. P., et al. 2003, in X-Ray and Gamma-Ray Telescopes and Instruments for Astronomy. Edited by J. E. Truemper, H. D. Tananbaum. Proceedings of the SPIE, Volume 4851, pp. 28-44 (2003)., 28–44
Hunter, D. A. & Gallagher, J. S. 1986, PASP, 98, 5
Hunter, D. A., Hawley, W. N., & Gallagher, J. S. 1993, AJ, 106, 1797
Kaper, L., et al. 1995, A&A, 300, 446
Kitamoto, S., Mizobuchi, S., Yamashita, K., & Nakamura, H. 1994, ApJ, 436, 418
Lequeux, J., et al. 1979, A&A, 80, 155
Liedahl, D. A. & Paerels, F. 1996, ApJ, 468, L33
Maeder, A. & Meynet, G. 1994, A&A, 287, 803
Massey, P. & Armandroff, T. E. 1995, AJ, 109, 2470
Massey, P., Armandroff, T. E., & Conti, P. S. 1992, AJ, 103, 1159
Massey, P. & Johnson, O. 1998, ApJ, 505, 793
McClintock, J. E. & Remillard, R. A. 2003, Review, Chap. 4
Mewe, R., Gronenschild, E. H. B. M., & van den Oord, G. H. J. 1985, A&AS, 62, 197
Predehl, P., Burwitz, V., Paerels, F., & Trümper, J. 2000, A&A, 357, L25
Roberts, T. P., Goad, M. R., Ward, M. J., & Warwick, R. S. 2003, MNRAS, 342, 709
Royer, P., Smartt, S. J., Manfroid, J., & Vreux, J.-M. 2001, A&A, 366, L1
Safi-Harb, S. & Oegelman, H. 1997, ApJ, 483, 868
Saha, A., Hoessel, J. G., Krist, J., & Danielson, G. E. 1996, AJ, 111, 197
Sakai, S., Madore, B. F., & Freedman, W. L. 1999, ApJ, 511, 671
Stark, A. A., et al. 1992, ApJS, 79, 77
Thronson, H. A., Hunter, D. A., Casey, S., & Harper, D. A. 1990, ApJ, 355, 94
Townsley, L. K., Broos, P. S., Nousek, J. A., & Garmire, G. P. 2002, Nuclear Instruments and Methods in Physics Research A, 486, 751
van Kerkwijk, M. H., et al. 1996, A&A, 314, 521
White, N. E., Nagase, F., & Parmar, A. N. 1995, in X-ray Binaries, ed. W. H. Lewin, J. Van Paradijs, & E. P. J. van den Heuvel (Cambridge: Cambridge University Press), p. 1
Yang, H. & Skillman, E. D. 1993, AJ, 106, 1448